Electronic Supplementary Information (ESI)

1. Experimental

1.1. Chemicals

Methyl ethyl ketone (MEK, >99%, Fisher Scientific), phenol (> 99%, Sigma-Aldrich), formaldehyde (ACS reagent, 37 wt% in H_2O, methanol stabilized, Sigma-Aldrich), sodium hydroxide (NaOH, >99%, EMD Chemicals), hydrochloric acid (HCl, >37%, Fluke Analytical), were used as received. The thermally crosslinkable phenolic resin oligomer (resol) served as a carbon precursor, and its preparation by using phenol and formaldehyde (37 wt% in H_2O) in a base-catalyzed (NaOH) process was previously reported.[1] The resol in MEK was stored in a refrigerator at 5-10 °C to minimize additional condensation and crosslinking prior to the thermopolymerization. The amphiphilic triblock copolymer template poly(ethylene oxide)-block-poly(ethyl acrylate)-block-polystyrene (PEO_{45}-b-PEA_{117}-b-PS_{99}) with M_n = 24 kDa and dispersity (Đ) = 1.2 was synthesized by reversible addition-fragmentation chain transfer (RAFT) polymerization. The synthetic routes and post characterization of PEO_{45}-b-PEA_{117}-b-PS_{99} was described in our previous publication.[2] PEO_{45}-b-PEA_{117}-b-PS_{99} (template) and resol (precursor) were dissolved in MEK to make 10 wt% solutions. Clean Silicon wafers (substrate) were prepared by placing them in UV ozone (Jelight Company Inc., Model No. 42) for 2 h.

1.2 Films Preparation and Processing

Thin-film samples were prepared on clean silicon wafers by spin-coating at 3000 rpm for 1 min from a 10 wt% MEK solution with mixture of PEO_{45}-b-PEA_{117}-b-PS_{99} and resol under different resol wt%. The films thickness varies from 500~620 nm depending on the resol content. Then the films were annealed with MEK vapor in a chamber using mass flow controllers (MKS-146C-FF000-1) in which the dry air was bubbled through MEK solvent to produce mixtures of saturated MEK vapor and dry air stream prior to entering the annealing chamber. The flow total rate of the streams was set constant at the 800 cm^3/min and the partial vapor pressure of MEK was controlled at approximately saturation. The volume of MEK solvent (25 mL) was sufficient to remain in the container for about 2 h under the flow rate utilized. To investigate the influence of SVA time and the film drying rate on film structure, two different SVA processing conditions, referred to as single SVA with fast drying and double SVA with slow drying, were employed. For the single SVA, the thin-film samples were solvent vapor annealed in MEK vapor for approximately 1 h and then the solvent reservoir was refilled (25 mL) and the same SVA conditions continued at ambient temperature with a direct taking off samples after 2 h; while for the double SVA, the samples were annealed in MEK vapor for over 3 h until dry, and then the solvent reservoir was refilled (25 mL) and the same SVA conditions continued until the sample was dried (>3 h additional SVA). Fig. S1 illustrates the time dependence

of the thickness of a film containing 25 wt.% resol as determined by in-situ spectroscopic ellipsometry (J.A Woollam Co., M-2000) at an incident angle of 70°. This clearly illustrates the initial swelling of the blend film by MEK vapor, an overshoot and relatively slow drying as the solvent in the reservoir is depleted. Note that there is no equilibrium swelling thickness obtained under the conditions utilized, which limits the effective SVA time during which the BCP and resol can re-organize. Following solvent vapor annealing (SVA), the films were heated at either 75 °C or 85 °C for 24 h to crosslink the resol to obtain thermopolymerized films. After that, the thermo-polymerized thin films were further heated at 400°C for 3 h in N_2 atmosphere to remove the template using a ramp rate of 1 °C/min. To fabricate the mesoporous carbon thin films, the calcined films were heated to 800 °C for 3 h at the heating rate of 1 °C/min below 400 °C and 4 °C/min above 400 °C.

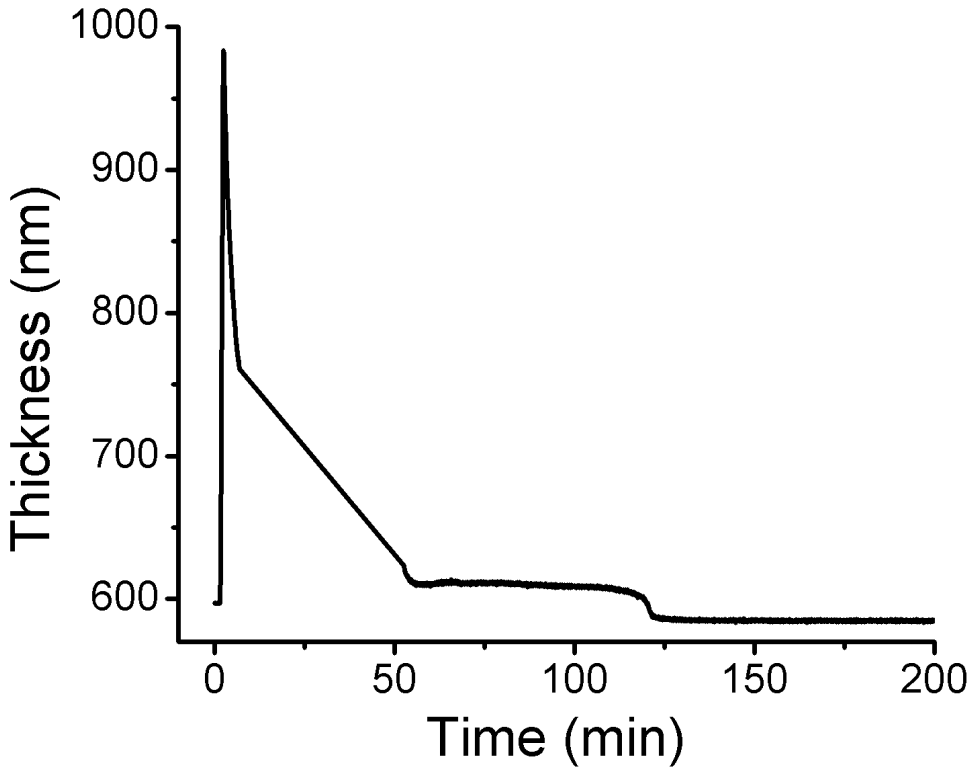

Fig. S1. Thickness evolution of 25 wt.% resol film during SVA as determined by in-situ spectroscopic ellipsometry.

1.3 Characterization of Thin Films

The thickness and optical properties (n, k) of the films were measured by a variable angle spectroscopic ellisometer (VASE, J.A Woollam Co., M-2000) using multiple incident angles (65°, 70° and 75°) over the wavelength from 246 nm to 1689 nm. A model containing the silicon substrate, a SiO_2 interface layer and a Cauchy layer was used to fit the obtained ellipsometric data. The porosity of the calcined films was calculated from the adsorption-desorption isotherm determined from the changes of

films' refractive index under the variations of partial pressure of probe solvent vapor (toluene). The partial pressure of the probe solvent was controlled by the same mass flow controllers as described for the SVA process.

Atomic force microscopy (AFM, Dimension ICON, Veeco) was employed to characterize the surface morphology of films in tapping mode at 0.5 Hz using PPP-NCC-50 tips (Nanosensors). Grazing incidence small angle X-ray scattering (GISAXS) was conducted to investigate the ordered structure of the films at the X9 beamline of the National Synchrotron Light Source (NSLS) at Brookhaven National Laboratory (BNL). The incident X-ray beam was 13.5 keV with wavelength (λ) = 0.0918 nm at a distance of 4.73 m from sample to detector. All GISAXS profiles were obtained both below and above the critical angle under vacuum.

2. Processing dependent morphology

The morphology of the films is strongly dependent on processing conditions. The initial cast films exhibit short range order irrespective of resol content as shown in Fig. S2. The surface morphology for all three resol contents (25 wt.%, 50 wt.% and 60 wt.%) illustrated appears to be poorly ordered cylinders.

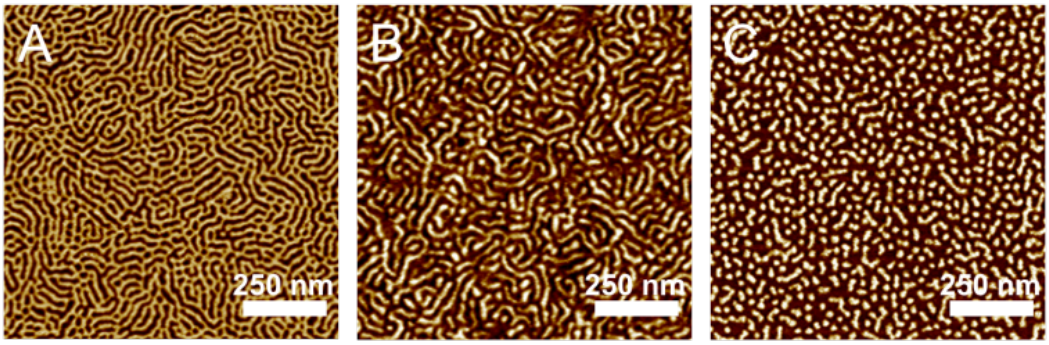

Fig. S2. AFM phase images of as-cast PEO_{45}-b-PEA_{117}-b-PS_{99}/resol films with growing resol content: (A) 25 wt.%; (B) 50 wt.%; (C) 60 wt.%. The resol was approximately 17 weeks old when the films were cast.

This morphology for the films can be significantly altered by solvent exposure as shown in Fig 1 using the single SVA procedure. However on heating the films after SVA, the structure significantly re-arranges even when low crosslinking temperature is utilized to minimize chain mobility and the highly ordered structures from SVA are lost. Fig S3 illustrates the relatively poorly ordered mesostructures obtained after thermopolymerization of films that were highly ordered by single SVA. The best ordered structure is the cylinders obtained at 50 wt.% resol (Fig. S3B), but this structure was initially wavy line structure after SVA (Fig. 1D). The thermally induced phase transitions in these films significantly hinder the ability to fabricate mesoporous films with the desired gyroid morphology.

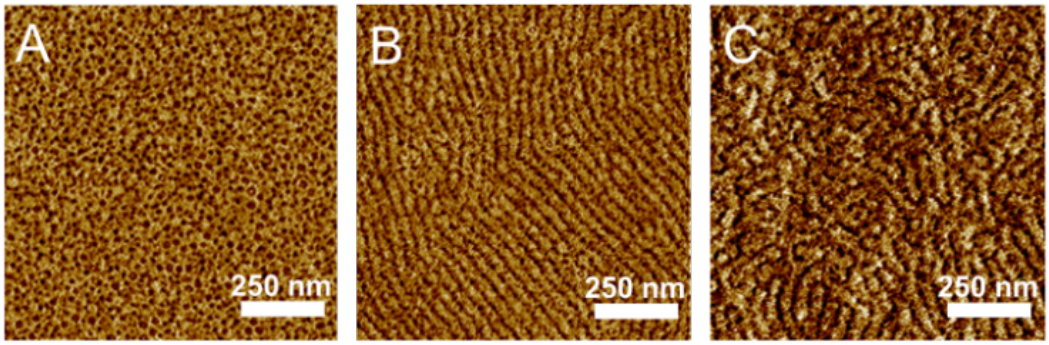

Fig. S3. AFM phase images of thermopolymerized films heated at 85 °C for 24 h after application of single SVA prior to thermopolymerization, containing (A) 25 wt.%; (B) 50 wt.%; (C) 60 wt.% resol. The resol was approximately 17 weeks old when the films were cast.

Additional information about the pore structure is determined using ellipsometric porosimetry (EP) for the films after template removal (calcined) as shown in Fig. S4A. The porosity and pore size distribution are determined using Lorentz-Lorentz effective medium approximation and Kelvin equation, respectively.[3, 4] These films exhibit the typical type IV adsorption-desorption isotherms of mesoporous materials. The porosity of these mesoporous gyroid is significantly greater (about 50 %) than typically observed in other ordered morphologies for mesoporous carbon films.[5, 6] The pore size distribution is broader than typically reported for ordered mesoporous materials as shown in Fig. S4B. It should be noted that the Kelvin equation is not strictly applicable to the gyroid structure, which may explain the inconsistency in pore size between AFM (around 12 nm) and the pore size determined by EP (approximately 30 nm).

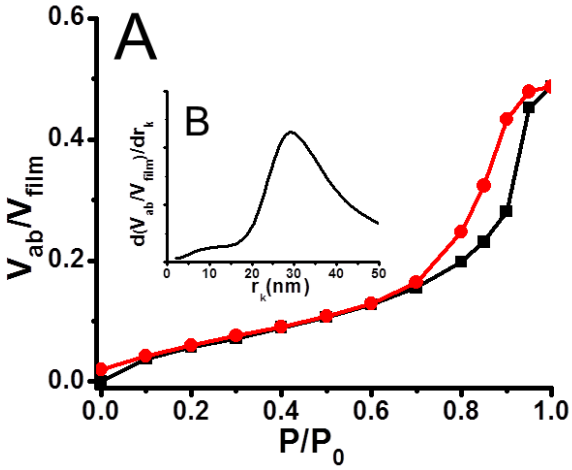

Fig. S4. (A) Adsorption (■) and desorption (●) isotherms of mesoporous calcined gyroid films (Fig 2C and Fig 3B) using toluene as probe solvent as determined by ellipsometric porosimetry. (B) Estimated pore size distribution determined from EP using the Kelvin equation.

3. Impact of resol age on morphology

In addition to the sensitivity to the SVA and resol content, the age of the resol can significantly alter the morphology obtained. By aging the resol by approximately an additional 6 mo. in a refrigerator at ~ 5 °C, the compositional window for the gyroid is shifted. As shown in Fig. S5, the gyroid is not obtained for the 25 wt.% resol film after the double SVA procedure with this aged resol, but instead perpendicularly oriented cylinders are obtained (Fig. S5A). However, increasing the resol content to nearly 29 wt.% results in the gyroid again, so the compositional window for the gyroid is shifted by 4 wt % compared with single SVA procedure along with aging (Fig. S5B). Of particular interest is the morphology of the 33.3 wt.% resol film, where the parallel cylinder (Fig. S5C) morphology transforms partially to gyroid structure (Fig. S5I) during thermopolymerization at 85 °C. This OOT phenomenon is very similar to that reported for the first double SVA with a young resol, except that the

resol content changes from 25.0 wt.% to 33.3 wt.%. This compositional shift for gyroid structure with aging is likely due to the extreme temperature sensitivity of the morphology as shown in Fig. S5 with the mesostructure after thermopolymerization at 75 °C and 85 °C being somewhat different. As the resol ages, the degree of polymerization increases, which shifts the degree of segregation (χN) for the cooperatively assembled blend. As the morphology is strongly temperature dependent, this suggests that the morphology should also be quite sensitive to small changes in the degree of segregation. Thus, repeatability of the gyroid structure also depends on specific details associated with the resol. However, the small size, broad molecular weight distribution associated with condensation and the difficulties with eluding resol through a standard GPC column (WARNING: we have ruined a column due to the near irreversible adsorption of resol to the packing material in THF. No peaks were seen for the resol using an RI detector, which makes quantifying the resol structure extremely challenging).

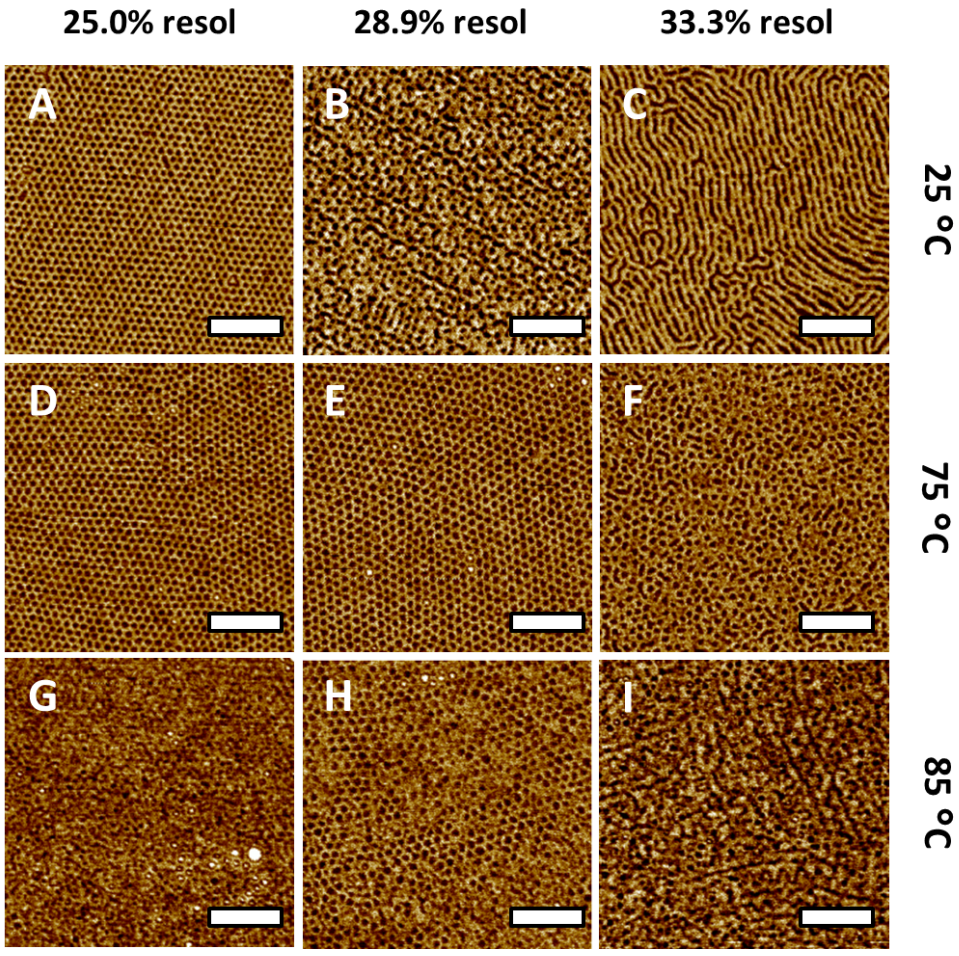

Fig. S5 AFM phase images of films using second double SVA procedure containing different resol content, at 25 °C, (A) 25.0 wt.%; (B) 28.9 wt.%; (C) 33.3 wt.%; and at 75 °C,; (D) 25.0 wt%; (E) 28.9 wt.%; (F) 33.3 wt.%; and (G) 25.0 wt.%; (H) 28.9 wt.%; (I) 33.3 wt.% after exposure to MEK using

double SVA (repeated work). (Scale bar: 250 nm.) The resol was approximately 34 weeks old when the films were cast.

For the 25 wt. % resol film (shown in Fig. S5A), the GISAXS profile above the critical angle is shown in Fig S6. The streaking is consistent with perpendicular cylinders. The higher order reflections at peaks at 0.236, 0.41, 0.47, 0.61, 0.71, and 0.83 nm^{-1} are approximately at a ratio of √1, √3, √4, √7, √9, etc. as would expected for perpendicular cylinders.

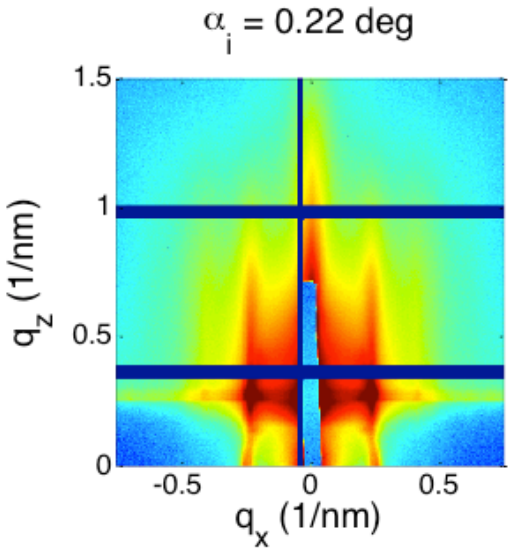

Fig. S6. GISAXS profile for 25 wt.% resol film after double SVA process obtained at an incident angle of 0.22°.

The gyroid morphology shown in Fig. S5B for the film with 28.9 wt.% resol can be confirmed by GISAXS as shown in Fig. S7.

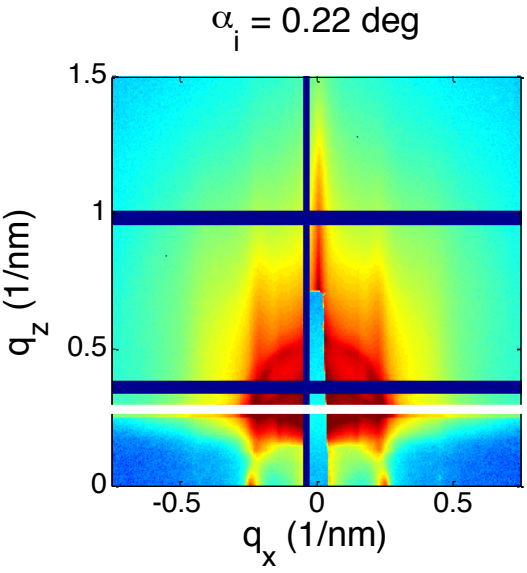

Fig. S7. GISAXS profile for 28.9 wt.% resol film after double SVA process obtained at an incident angle of 0.22°.

To better illustrate the multiple peaks associated with the gyroid morphology, a line cut (white stripe in Fig. S7 around q_z = 0.25 nm^{-1}) is utilized to obtain the relation between intensity diffraction peaks with q_x. The diffraction peaks associated with the double gyroid morphology are shown in Fig. S8. Five orders of diffraction are clearly visible in this 1-D profile; sharp peaks are visible at approximately 0.138, 0.194, 0.226, and 0.270 nm^{-1}, while broad peaks are observed near 0.438 nm^{-1}. These peaks from the line scan correspond to reflection ratios of $\sqrt{2}$, $\sqrt{4}$, $\sqrt{6}$, $\sqrt{8}$, $\sqrt{20}$. The double gyroid should exhibit peaks at $\sqrt{6}$, $\sqrt{8}$, $\sqrt{20}$. We attribute the additional peaks at $\sqrt{2}$ and $\sqrt{4}$ to a slight distortion in the gyroid lattice due to constraints of the substrate during the solvent removal. Distortion in the gyroid lattice is known to allow for typically 'forbidden' reflections.[7,8]

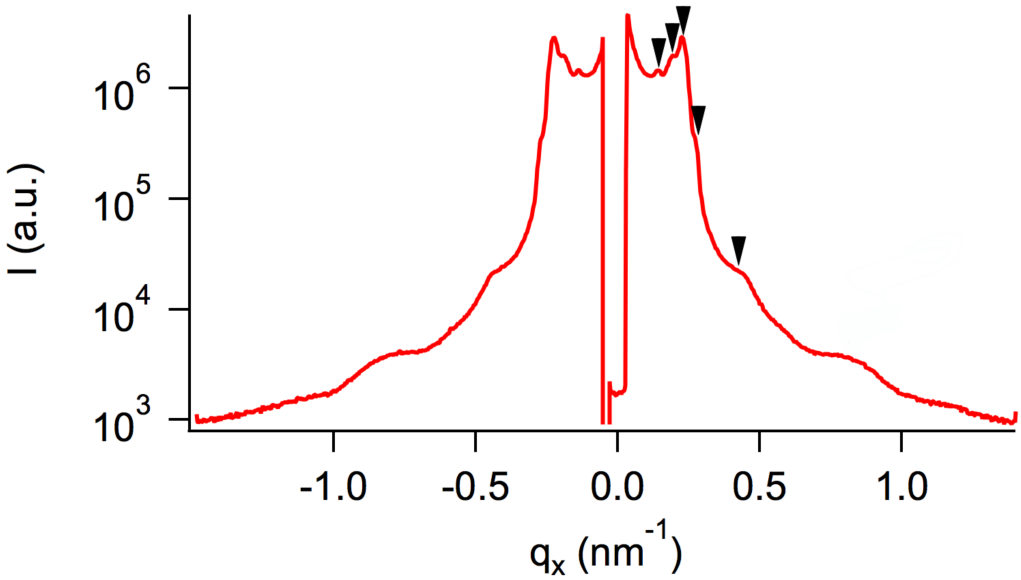

Fig. S8. Line cut in q_x of the GISAXS profile shown in Fig. S7. The series of peaks at low q are consistent with a slightly deformed gyroid space group.

References

1. Y. Meng, D. Gu, F. Q. Zhang, Y. F. Shi, H. F. Yang, Z. Li, C. Z. Yu, B. Tu and D. Y. Zhao, *Angew. Chem. Int. Ed.*, 2005, **44**, 7053-7059.
2. G. Deng, Z. Qiang, W. Lecorchick, K. A. Cavicchi and B. D. Vogt, *Langmuir*, 2014, **30**, 2530-2540.
3. M. R. Baklanov, K. P. Mogilnikov, V. G. Polovinkin and F. N. Dultsev, *J. Vac. Sci. Technol. B.*, 2000, **18**, 1385-1391.

4. J. Dendooven, K. Devloo-Casier, E. Levrau, R. Van Hove, S. P. Sree, M. R. Baklanov, J. A. Martens and C. Detavernier, *Langmuir*, 2012, **28**, 3852-3859.
5. L. Y. Song, D. Feng, N. J. Fredin, K. G. Yager, R. L. Jones, Q. Y. Wu, D. Y. Zhao and B. D. Vogt, *ACS Nano*, 2010, **4**, 189-198.
6. X. X. Li, A. B. Larson, L. Jiang, L. Y. Song, T. Prichard, N. Chawla and B. D. Vogt, *Micropor. Mesopor. Mat.*, 2011, **138**, 86-93.
7. E. J. W. Crossland, M. Kamperman, M. Nedelcu, C. Ducati, U. Wiesner, D. M. Smilgies, G. E. S. Toombes, M. A. Hillmyer, S. Ludwigs, U. Steiner and H. J. Snaith, *Nano Lett.*, 2009, **9**, 2807-2812.
8. V. N. Urade, T.-C. Wei, M. P. Tate, J. D. Kowalski and H. W. Hillhouse, *Chem. Mater.*, 2007, **19**, 768-777.